IJHSR
ijhighschoolresearch.org
RESEARCH ARTICLE

Selective Inhibition of MMP-2 Protein for Preventing Decorin Cleavage Linked with Hypermobile Ehlers-Danlos Syndrome

Shreejith Krishnamoorthy

Central Bucks High School South, 1100 Folly Road, Warrington, Pennsylvania, 18976, USA; krishnamoorthyshreejith@gmail.com
Mentor: Ryan Ford

ABSTRACT: Hypermobile Ehlers-Danlos Syndrome (hEDS), a connective tissue and joint disorder that affects millions of people, causes chronic pain, increases the risk of injury, and other diseases. Up to 25% of the world population is also predicted to be affected by this condition in the future, making targeted therapeutics essential. Recent discoveries in the methylenetetrahydrofolate biological pathway associated with hEDS have enabled this study to attempt to develop targeted therapeutics. This study leverages and develops the rationale behind the inhibition of the matrix metalloprotease-2 (MMP-2) enzyme to act as a therapy for hEDS. Small molecule inhibitors were chosen for the mode of inhibition due to ease of production, effectiveness, and analysis. Identification of top inhibitors/drug candidates for MMP-2 was conducted *in silico* utilizing thermochemical and structural metrics computed in Maestro, a computational chemistry software. Drug candidates were also sorted based on the biological and cellular context of the disease rather than just potency. The top inhibitor, ChemBridge 3040, is predicted to have a binding affinity of -80.93 kilocalories per mole to the binding site of MMP-2. Experimental validation of the drug targets required recombinant MMP-2 expression. Two novel expression cultures were developed to validate *in vitro* efficacy.

KEYWORDS: Chemistry, Computational Chemistry, Protein Inhibitors, Protein Expression, Matrix Metalloproteinase.

Introduction

Hypermobile Ehlers-Danlos Syndrome (hEDS) is a connective tissue and joint disorder that is diagnosed in 1 in 500 people globally and is predicted to affect up to 25% of people in an undiagnosed and mild manner.[1,2] Inflicted patients suffer from chronic muscular and bodily pain; increased risk of injury and disease; loss of connective tissue function; joint pain/instability; and various other complications.[3] Primarily caused by genetic mutations and inherited through family lineages, the incidence of hEDS cases is steadily increasing. Despite the increasing need for therapeutics, there are currently no targeted therapies—only retrospective painkillers and vitamin supplements.[4,5]

The predominant mutation in hEDS patients is the suppression of the methylenetetrahydrofolate reductase (MTHFR) gene, resulting in haltered expression of the MTHFR enzyme.[6] Metalloprotease-2 (MMP-2) is an enzyme that aids in the catalysis of cleavage within various extracellular matrix (ECM) peptides and proteins. Recent discoveries have heavily associated MMP-2 with a complex biological pathway involved in the advancement of hEDS.[7]

Typically, MTHFR would catalyze a reaction to form 5-methylenetetrahydrofolate (5-MTHF) from 10-methylenetetrahydrofolate (10-MTHF), as seen in Figure 1.[7]

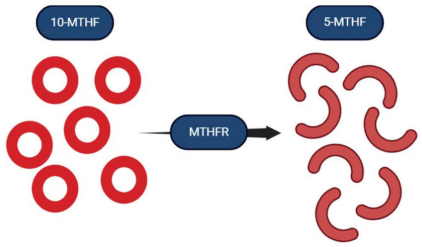

Figure 1: Visualization of the MTHFR enzyme cleaving the 10-MTHF vitamin into the 5-MTHF vitamin.

5-MTHF would subsequently inhibit the MMP-2 enzyme. This inhibition would result in an organized extracellular matrix (ECM) and inactivated fibroblast, a cell mechanism responsible for injury repair, as seen in Figure 2.[7]

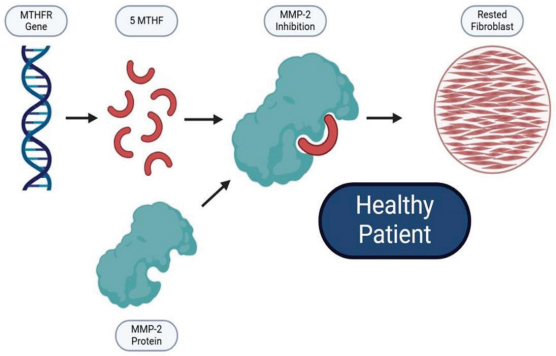

Figure 2: Visualization of the MTHFR gene mechanism, the MTHFR gene produces MTHFR, which produces 5-MTHF, which then inhibits the MMP-2 enzyme, leading to proper regulation of the debris in the ECM and resting fibroblast.

Downregulation mutations in the MTHFR gene, found in hEDS patients, result in reduced MTHFR expression, leading

DOI: 10.36838/v8i3.76

to the reduced production of 5-MTHF. This allows MMP-2 to be overactivated and cleave decorin, a peptide that increases the availability of transforming growth factor β (TGFβ) and thus, activates fibroblasts without any injury to repair. This leads to fibrosis, which is the scarring and damage of tissue caused by falsely activated fibroblasts, as seen in Figure 3.[7]

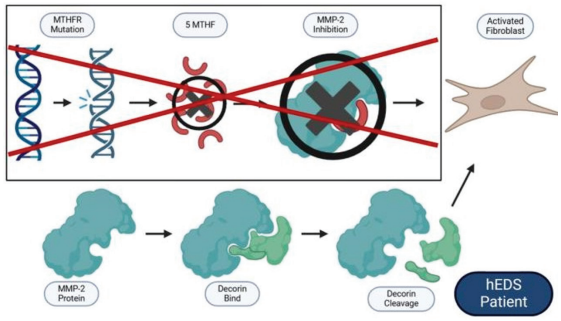

Figure 3: Visualization of the downregulated MTHFR gene mechanism, the MTHFR gene produces less MTHFR, which produces less 5-MTHF, which then cannot inhibit the MMP-2 enzyme, leading to MMP-2 cleaving decorin, resulting in increased TGFβ and, in turn, activating fibroblast or inducing fibrosis.

The mechanism described above allows the supplementation of 5-MTHF to be a possible therapeutic for hEDS. However, clinical supplementation of this compound had minimal to no results.[7] Further analysis determined that another biological process involving methionine synthase actively converts 5-MTHF into 10-MTHF, reducing its efficacy drastically, as seen in Figure 4.[7]

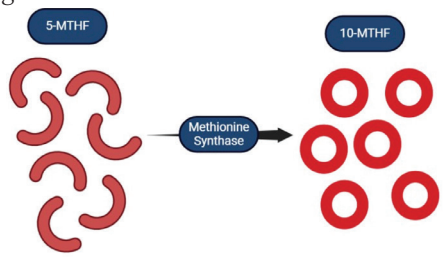

Figure 4: Visualization of the methionine synthase mechanism, methionine synthase catalyzes a reaction to form 10-MTHF from 5-MTHF.

As a method to counteract these results, testing synthetic inhibitors of MMP-2 could prove to be an effective therapeutic for hEDS. These inhibitors would be selective yet unique, allowing them to inhibit MMP-2 without being catalyzed by methionine synthase, as seen in Figure 5.

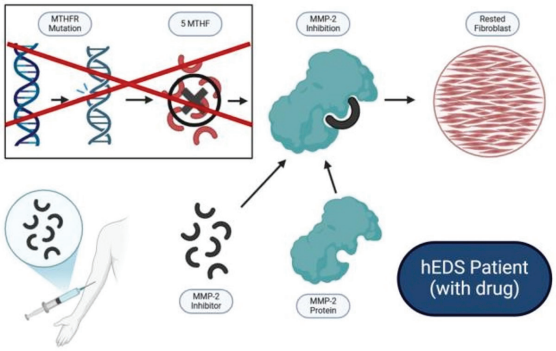

Figure 5: Visualization of the downregulated MTHFR gene mechanism with the proposed MMP-2 inhibitors as drug candidates, the synthetic MMP-2 inhibitors could compensate for the reduced 5-MTHF production by inhibiting MMP-2 and returning normal function in the ECM.

Methods

Methods Overview:

The basic procedure of the experiment consisted of 3 main phases as follows: MMP-2 Protein Expression, Computational Inhibitor Screening, and Experimental/Activity Assays (Figure 6).

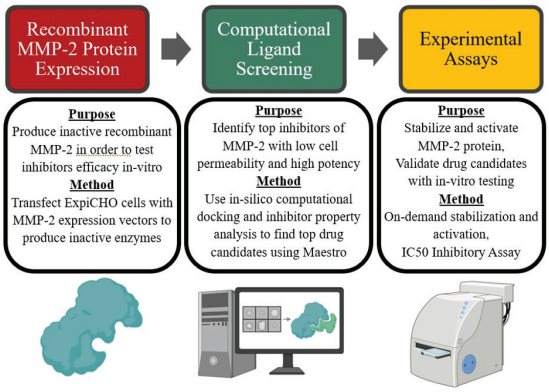

Figure 6: Methodology phases are separated into Recombinant MMP-2 Protein Expression, Computational Ligand Screening, and Experimental Assays, with purposes and methodologies briefly described.

Expression of Recombinant MMP-2 Enzyme:

Validation of potential inhibitors of the MMP-2 protein could only be done utilizing *in vitro* testing. MMP-2 protein could not be obtained from patient donors due to logistical and legal constraints. Replication of *in vivo* activity could be shown through recombinantly expressed proteins. The study utilized Expi Chinese Hamster Ovary (ExpiCHO™) cells and protocols to produce MMP-2 using two distinct expression vectors, recombinant DNA used to produce protein.[8] CAUTION: The mentioned methods and protocols can expose individuals to biological, chemical, and mechanical hazards.

In-vivo expression of the MMP-2 protein produces a propeptide region along with the protein itself to fold it properly, so recombinant expression vectors were ordered with the propeptide amino acid sequence along with the protein amino acid sequence. The propeptide region keeps the MMP-2 enzymatically inactive until cleaved using the membrane type 1 matrix metalloproteinase (MT1-MMP) enzyme *in vivo* (Figure 7).[9] However, with no access to MT1-MMP, the study mutated the amino acid sequence to include a Furin enzyme cleavage site (RAKR) since the study had access to Furin (Figure 8).[10] This resulted in the study producing two separate MMP-2 proteins, one with the wild-type amino acid sequence known as MMP-2-Native and one with the Furin cleavage site implemented between the propeptide sequence and the MMP-2 protein sequence (Table 1). The study chose to produce MMP-2-Native even though MT1-MMP was not available, since there are possibilities of autocatalysis and autoactivation, which would not require MT1-MMP. Furthermore, MMP-2-Furin could alter the protein's structure, resulting in a completely different protein, so MMP-2-Native was produced as a backup.

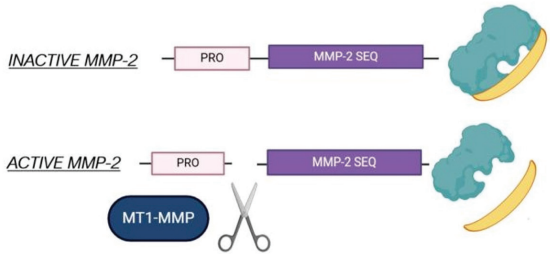

Figure 7: Visualization of *in vivo* activation of MMP-2, MMP-2 remains inactive until MT1-MMP cleaves off the propeptide sequence.

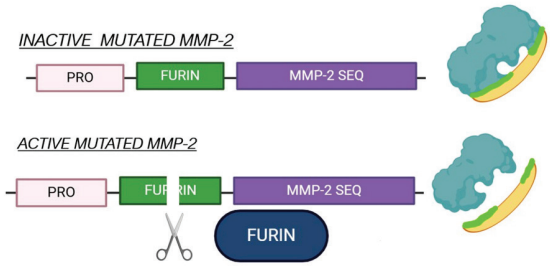

Figure 8: Visualization of suggested *in vitro* activation of MMP-2, MMP-2 remains inactive until Furin cleaves off the propeptide using the Furin cleavage site, which was implemented.

Table 1: The table displays the two variants of MMP-2, which will be produced in this study, along with the plasmid amino acid sequence color-coded by each segment of the protein, labeled in the notes section.

MMP-2-Native and MMP-2-Furin Amino Acid Sequence

MMP-2 Variant	Amino Acid Sequence
MMP-2-Native	MGVKVLFALICIAVAEAAPSPIIKFPGDVAPKTDKELAVQYLNTFY GCPKESCNLFVLKDTLKKMQKFFGLPQTGDLDQNTIETMRKPRCGN PDVANYNFFPRKPKWDKNQITYRIIGYTPDLDPETVDDAFARAFQV WSDVTPLRFSRIHDGEADIMINFGRWEHGDGYPFDGKDGLLAHAFA PGTGVGGDSHFDDDELWTLGEGQVVRVKYGNADGEYCKFPFLFNGK EYNSCTDTGRSDGFLWCSTTYNFEKDGKYGFCPHEALFTMGGNAEG QPCKFPFRFQGTSYDSCTTEGRTDGYRWCGTTEDYDRDKKYGFCPE TAMSTVGGNSEGAPCVFPFTFLGNKYESCTSAGRSDGKMWCATTAN YDDDRKWGFCPDQGYSLFLVAAHAFGHAMGLEHSQDPGALMAPIYT YTKNFRLSQDDIKGIQELYGASPD**H6**
MMP-2-Furin	MGVKVLFALICIAVAEAAPSPIIKFPGDVAPKTDKELAVQYLNTFY GCPKESCNLFVLKDTLKKMQKFFGLPQTGDLDQNTIETMRKPRCGN P**RAKR**YNFFPRKPKWDKNQITYRIIGYTPDLDPETVDDAFARAFQV WSDVTPLRFSRIHDGEADIMINFGRWEHGDGYPFDGKDGLLAHAFA PGTGVGGDSHFDDDELWTLGEGQVVRVKYGNADGEYCKFPFLFNGK EYNSCTDTGRSDGFLWCSTTYNFEKDGKYGFCPHEALFTMGGNAEG QPCKFPFRFQGTSYDSCTTEGRTDGYRWCGTTEDYDRDKKYGFCPE TAMSTVGGNSEGAPCVFPFTFLGNKYESCTSAGRSDGKMWCATTAN YDDDRKWGFCPDQGYSLFLVAAHAFGHAMGLEHSQDPGALMAPIYT YTKNFRLSQDDIKGIQELYGASPD**H6**

Note. RAKR = furin cleavage site - MMP2 propeptide - MMP2 catalytic domain - His6 tag

Table 2: The table displays the amino acid sequence of both MMP-2 Native and MMP-2 Furin, which have been aligned against each other to emphasize the differences.

```
Native 1    MGVKVLFALICIAVAEAAPSPIIKFPGDVAPKTDKELAVQYLNTFYGCPKESCNLFVLKD  60
Furin  1    MGVKVLFALICIAVAEAAPSPIIKFPGDVAPKTDKELAVQYLNTFYGCPKESCNLFVLKD  60

Native 61   TLKKMQKFFGLPQTGDLDQNTIETMRKPRCGNPDVANYNFFPRKPKWDKNQITYRIIGYT  120
Furin  61   TLKKMQKFFGLPQTGDLDQNTIETMRKPRCGNPRAKRYNFFPRKPKWDKNQITYRIIGYT  120

Native 121  PDLDPETVDDAFARAFQVWSDVTPLRFSRIHDGEADIMINFGRWEHGDGYPFDGKDGLLA  180
Furin  121  PDLDPETVDDAFARAFQVWSDVTPLRFSRIHDGEADIMINFGRWEHGDGYPFDGKDGLLA  180

Native 181  HAFAPGTGVGGDSHFDDDELWTLGEGQVVRVKYGNADGEYCKFPFLFNGKEYNSCTDTGR  240
Furin  181  HAFAPGTGVGGDSHFDDDELWTLGEGQVVRVKYGNADGEYCKFPFLFNGKEYNSCTDTGR  240

Native 241  SDGFLWCSTTYNFEKDGKYGFCPHEALFTMGGNAEGQPCKFPFRFQGTSYDSCTTEGRTD  300
Furin  241  SDGFLWCSTTYNFEKDGKYGFCPHEALFTMGGNAEGQPCKFPFRFQGTSYDSCTTEGRTD  300

Native 301  GYRWCGTTEDYDRDKKYGFCPETAMSTVGGNSEGAPCVFPFTFLGNKYESCTSAGRSDGK  360
Furin  301  GYRWCGTTEDYDRDKKYGFCPETAMSTVGGNSEGAPCVFPFTFLGNKYESCTSAGRSDGK  360

Native 361  MWCATTANYDDDRKWGFCPDQGYSLFLVAAHAFGHAMGLEHSQDPGALMAPIYTYTKNFR  420
Furin  361  MWCATTANYDDDRKWGFCPDQGYSLFLVAAHAFGHAMGLEHSQDPGALMAPIYTYTKNFR  420

Native 421  LSQDDIKGIQELYGASPDHHHHHH  444
Furin  421  LSQDDIKGIQELYGASPDHHHHHH  444
```

The protein was purified using the His-6 tag at the end of the protein and immobilized metal affinity chromatography (IMAC) as stated in well-known protocols.[11] To ensure that the protein produced was indeed MMP-2-Native and MMP-2-Furin, a protein Ultraviolet (UV) Scan and a sodium dodecyl sulfate-polyacrylamide gel electrophoresis (SDS-PAGE) were conducted according to well-established protocols.[12,13]

Computational Identification of Synthetic Inhibitors of MMP-2:

Identification of effective inhibitors manually through trial-and-error processes is time-consuming, ineffective, and expensive. As a result, the study utilized a computational chemistry program called Maestro to computationally identify the best inhibitors for the MMP-2 protein. Maestro was the only computational chemistry software available for the study. Various arrays of analysis were used. The ligands that were tested come from a bank of 150,000 compounds that are available for use in the study. The purpose is to find inhibitors with low IC50 values. (Inhibitory Concentration 50%)—a metric of inhibitory potency.

The study strategically filtered through the 150,000 compound library using a workflow that is shown in Figure 9. The figure will include the number of compounds the study expects to remain in each section of the workflow. Refer to the Maestro resource catalog for specific information (such as methodology and protocols) on any specific section.[14]

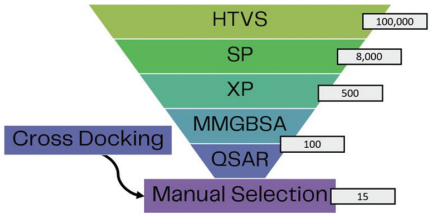

Figure 9: Visualization of computational workflow for filtering compounds with the highest predicted inhibitory potency in Schrodinger Maestro's application.

The computational workflow, which was used to identify drug candidates, can be seen in a visual representation above in Figure 9.

High Throughput Virtual Screening (HTVS): Screens 150,000 compounds and eliminates 50,000 compounds based on the physical size of the compound in comparison to the active site of the protein, i.e., whether the compound is too large or too small for the active site.[14]

Standard Precision (SP) Docking: Screens 100,000 compounds and eliminates 92,000 compounds based on predicted thermochemical favorability presented as a docking score (the more negative, the more thermochemically favorable). This metric is produced through computational rigid pose docking, rigidly placing various compounds in the active site and predicting the various forces of attraction and repulsion (hydrogen bonds, pi-cation bonds, etc.).[14]

Extra Precision (XP) Docking: Screens 8,000 compounds and eliminates 7,500 based on docking scores similar to SP Docking, however, with more computational power and time provided.[14]

DOI: 10.36838/v8i3.76

Molecular Mechanics Generalized Born Surface Area (MMGBSA) Solvation Model: Screens 500 compounds and eliminates 400 compounds based on thermochemical favorability presented as a ΔG Bind Score (the more negative, the more thermochemically favorable). The ΔG Bind Score is expressed in kcal/mol of reaction. This metric is produced through computational dynamic free binding docking, which allows the protein and the compound to rotate and move (similar to in-vivo expectations) and records the various forces of attraction and repulsion (hydrogen bonds, pi-cation bonds, etc.).[14]

Quantitative Structure Activity Relationship (QSAR): Creates a Machine Learning Model given known inhibitors of MMP-2 in order to predict the IC50 values of screened compounds. Around 6,000 known MMP-2 Inhibitors were used to generate this model. All 100 remaining compounds had IC50 values predicted for them.[14]

Manual Selection: 15 compounds were chosen based on the cell permeability of the compound and the QSAR-generated IC50 value.[14,15]

The study utilized the crystal structure and control inhibitor for the computational analysis from the Protein Data Bank (access code: 7XGJ) for all computational analyses.[16] The known inhibitor cited in the paper was also isolated and screened through the workflow above for control validation.[16] This control was chosen because it was one of the few inhibitors of the MMP-2 protein, which had recorded crystal structures in complex with MMP-2.

In Vitro Experimental Assays of MMP-2-Furin and MMP-2-Native:

In order to prepare the recombinantly produced proteins for an IC50 Assay, the study needs to ensure that the proteins produced are stable and enzymatically active.[17] The study chose to use a Thermal Shift Assay to determine the protein's stability through the proxy of how rapidly it denatures using well-documented protocols.[18] The study then chose to activate a portion of the MMP-2-Furin protein using 1 μL of 1 μM sample active Furin and incubate the sample at 32 degrees Celsius for 30 minutes. After that, an enzymatic activity assay was set up to determine whether the activated MMP-2-Furin was indeed active according to a well-documented protocol.[19-20] The specific substrate that the study chose was the MMP-2/MMP-7 Fluorogenic Substrate due to easy access and relatively cost-efficient pricing.[21]

The study aimed to run an IC50 Assay using active MMP-2 and all 15 identified compounds to determine the best-performing drug candidate for further experimentation.[17]

■ Result and Discussion

Expression of Recombinant MMP-2 Enzyme: Results:

After producing and purifying both MMP-2-Furin and MMP-2-Native proteins using well-known protocols elaborated on in the methodology portion of the paper, the purified protein was analyzed using a UV absorbance scan and an SDS-PAGE gel, respectively. The UV absorbance scan initially validated that the study successfully purified the protein at high concentrations. As seen in Figures 9 and 10, the UV Absorbance scan measured the amount of light absorbed at various wavelengths. Typically, all proteins absorb light at 280 nanometers. Both MMP-2-Native (Figure 10) and MMP-2-Furin (Figure 11) had multiple fractions that had high absorbance at the 280-nanometer mark, indicating a high concentration of protein.

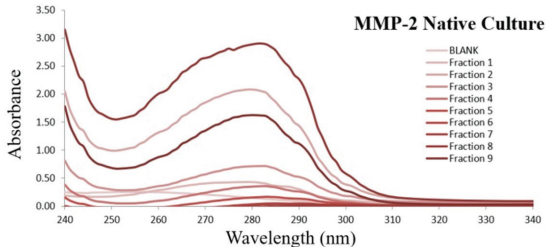

Figure 10: This graph shows the absorbance of 10 different protein fractions of the MMP-2-Native protein culture at different wavelengths. The graph shows that multiple fractions of protein have high absorbance at 280 nanometers, indicating that there is sufficient protein in this purified culture of MMP-2-Native.

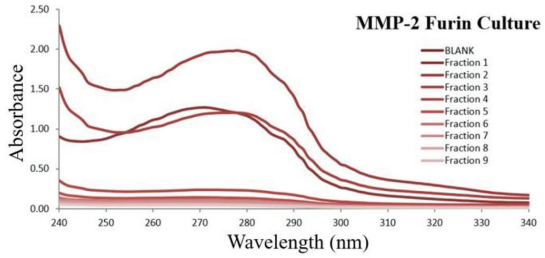

Figure 11: This graph shows the absorbance of 10 different protein fractions of the MMP-2-Furin protein culture at different wavelengths. The graph shows that multiple fractions of protein have high absorbance at 280 nanometers, indicating that there is sufficient protein in this purified culture of MMP-2-Furin.

After validating that both purified protein cultures have protein, the study chose to validate that the protein was indeed MMP-2-Native and MMP-2-Furin by conducting an SDS-PAGE gel, which would reveal the molecular weight of the protein tested. If the study successfully produced MMP-2-Native and MMP-2-Furin, then the SDS-PAGE will indicate that the molecular weight of both proteins would be around 50 kilodaltons.[16] The SDS-PAGE for both MMP-2-Native and MMP-2-Furin is shown below in Figure 12 and Figure 13, respectively.

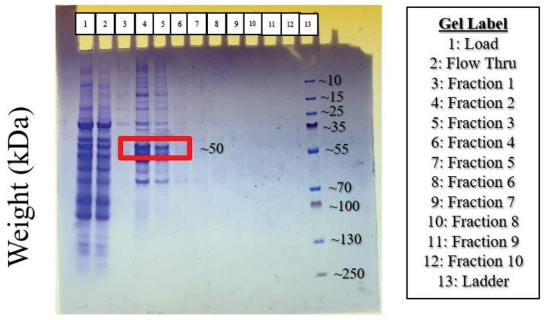

Figure 12: This graph shows the molecular weight of the MMP-2-Native protein culture to be around 50 kilodaltons for fractions 4 and 5 when compared against the protein weight ladder, which shows various milestones of weight in kilodaltons. This validates that the MMP-2-Native culture expressed is MMP-2.

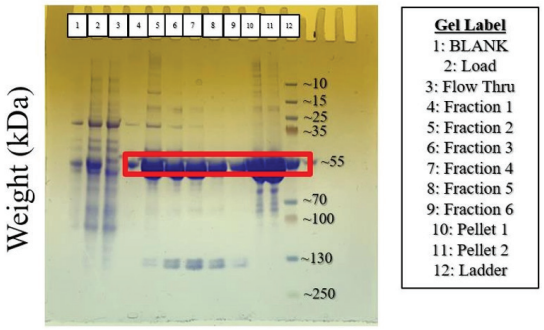

Figure 13: This graph shows the molecular weight of the MMP-2-Furin protein culture to be around 50 kilodaltons for fractions 4 through 12 when compared against the protein weight ladder, which shows various milestones of weight in kilodaltons. This validates that the MMP-2-Furin culture expressed is MMP-2.

The study successfully produced the MMP-2 protein in fractions 4 and 5 in the MMP-2-Native culture and in fractions 4 through 12 in the MMP-2-Furin culture. Fractions 4 and 5 were consolidated into a master stock for MMP-2-Native. Fractions 4 through 12 were consolidated into a master stock of protein for MMP-2-Furin. The concentration of the MMP-2-Native and MMP-2-Furin cultures was determined through a UV nanodrop with well-known protocols for more precision than the typical UV absorbance scan.[22] The nanodrop revealed that the MMP-2-Native and MMP-2-Furin had concentrations of 3.87 milligrams/milliliter and 3.96 milligrams/milliliter, respectively.

From the two SDS-PAGE gels that were conducted, it can be concluded that the two protein samples have molecular weights of approximately 50 kilodaltons, the theoretical weight of MMP-2. Although there are clear, concentrated markings at the desired protein weight markings for both proteins, the various erroneous markings can indicate impurities that may affect the further downstream end of experimentation on these proteins.

Computational Identification of Synthetic Inhibitors of MMP-2: Results:

After conducting all phases of the computational workflow cited in the methodology, the study narrowed down 15 compounds that have a high likelihood of being successful inhibitors for MMP-2 and, in turn, a successful drug candidate for hEDS. The top 15 compounds with their respective name designations, XP docking scores, and MM-GBSA binding affinity scores can be seen below in Table 3.

Table 3: The table displays 15 top compounds that were computationally identified to be potent inhibitors for the MMP-2 protein. This data was attained through computational chemistry metrics identified and explained in the methodology portion.

Compound	XP Docking Score	MM-GBSA Binding Affinity (kcal/mol)
5871-1859	-10.330	-45.42
ChemBridge.3040	-12.454	-44.94
BAS 0649085	-10.324	-44.90
BAS 2282287	-10.302	-43.73
BAS 2825385	-12.469	-42.69
BAS 1538434	-10.803	-41.58
ASN 3794129	-10.806	-36.65
4180-0304	-10.176	-35.00
Y200-1346	-10.371	-34.84
ChemBridge.14986	-11.092	-34.50
ChemBridge.11749	-11.141	-33.14
BTB 14099	-10.256	-33.07
3664-0103	-12.236	-33.00
BAS 0791468	-10.735	-32.85
4358-2895	-10.628	-31.97

When looking at various poses (physical positions in correspondence to the binding site) of all 15 compounds, the top compound, 5871-1859, had poses that seemed improbable, as well as many aromatic rings, which make it a larger compound, making it unideal. Due to those reasons, ChemBridge 3040 was considered the top inhibitor for this study. ChemBridge 3040's position, as well as the various bonds that occur while inhibiting MMP-2, visualized by Maestro, can be seen below in Figure 14.

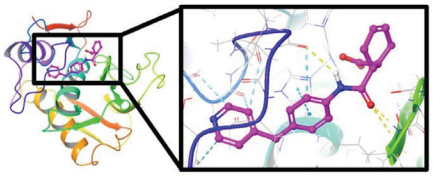

Figure 14: This visualization showcases the MMP-2 protein (rainbow) in complex with the top inhibitor Chembridge 3040 (pink). The various bonds (hydrogen, aromatic, etc.) are also showcased.

The individual compound of ChemBridge 3040 can also be seen isolated alone in Figure 15 below.

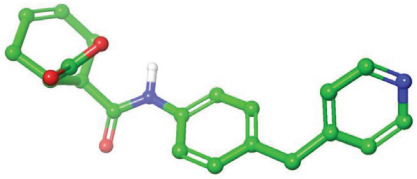

Figure 15: This visualization showcases the ChemBridge 3040 compound with carbons identified in green, nitrogens in blue, oxygens in red, and polar hydrogens in white. Non-polar hydrogens are not displayed.

The interactions between ChemBridge 3040 and the MMP-2 protein can be further analyzed in a ligand interac-

DOI: 10.36838/v8i3.76

tion diagram, shown below in Figure 17. The diagram labels can be seen in Figure 16.

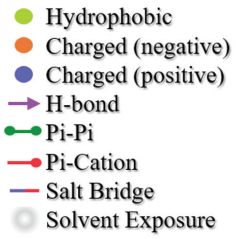

Figure 16: This figure shows the diagram labels for the following ligand interaction diagrams between inhibitory compounds and the MMP-2 protein.

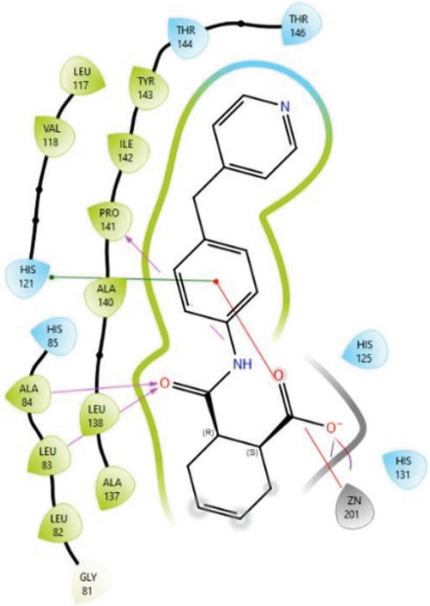

Figure 17: This figure is a ligand interaction diagram between MMP-2's various amino acids and ChemBridge 3040, which was the top inhibitor identified in this study. Please refer to Figure 16 for diagram labels.

As a comparison to ChemBridge 3040, the study also developed a ligand interaction diagram for the control inhibitor, which was identified in the methodology section. This control inhibitor ligand interaction diagram can be seen below in Figure 18.

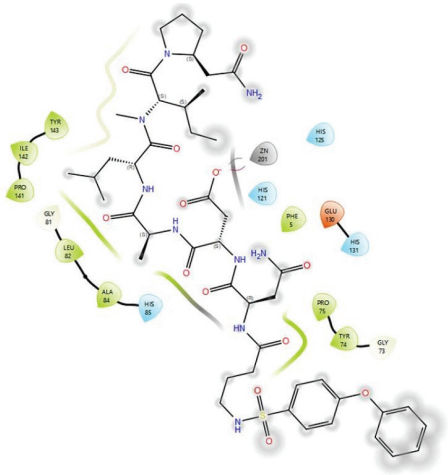

Figure 18: This figure is a ligand interaction diagram between MMP-2's various amino acids and the control inhibitor, which was identified previously by other researchers. Please refer to Figure 15 for diagram labels.

The QSAR Model was created from 6,000 MMP-2 inhibitors.[23] The model was trained to predict the IC50 value for MMP-2 of given compounds. The model used 75% of the dataset to train the model, and 25% of the dataset was used to test the accuracy. The model was deemed sufficiently accurate with an r^2 value of 0.91. A visualization of the model can be seen below in Figure 19.

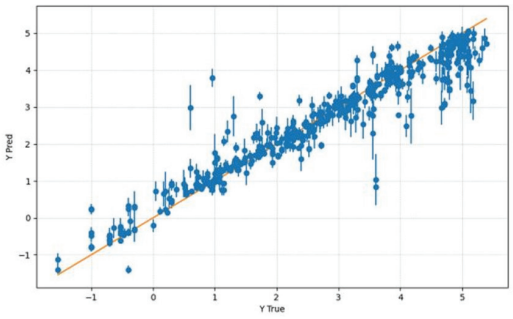

Figure 19: This figure is a graph of the predicted IC50 value of various inhibitors on the Y axis and the experimental IC50 values of the very same inhibitors. The prediction model is represented by the line of best fit shown in yellow.

The model predicted that ChemBridge 3040 would have an IC50 value of 7.877 x 10^{-5} nanomolar. This would be much more potent compared to the control inhibitor's IC50 value of 0.20 nanomolar.

The study then used SwissADME properties to determine the cell permeability of the top compound in comparison to the control inhibitor. A half-boiled egg plot can represent permeability, the ability to pass through various materials, by placing the compound as a point on the plot. The plot has a gray outer region, which represents impermeability through most biological barriers, including the gastrointestinal tract, which is how drugs are typically delivered. The inner white region, as well as the inner yellow region, represents gastrointestinal permeability, meaning that the compound has the potential to be delivered as a drug orally. The innermost yellow region also means that the compound can pass through the blood-brain barrier and can act as a proxy for cell membrane permeability. Since MMP-2 is an extracellular protein, the ideal range for the MMP-2 inhibitory compound is in white since it will be a deliverable drug yet not too permeable such that it permeates cells unnecessarily. Figure 20 below shows the half-boiled egg plot with the top and control compound.

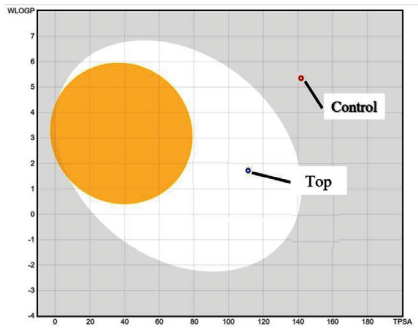

Figure 20: This figure is a graph of the WLOGP on the y axis, which is the octanol-water partition coefficient, which can predict a compound's lipophilicity, and TPSA on the x axis, which is the topological polar surface area, which, in combination with the WLOGP, can predict bioavailability as described above.

The control inhibitor can be seen in the gray area, meaning that the compound is not permeable through the gastrointestinal tract. The top inhibitor, ChemBridge 3040, can be seen in the white region of the graph, meaning that the compound is the ideal permeability that the study sought after in MMP-2 inhibitors.

All these factors indicate that ChemBridge 3040 will be a better inhibitor for this study in comparison to the control inhibitor.

In Vitro Experimental Assays of MMP-2-Furin and MMP-2-Native:

The stability of MMP-2-Native and MMP-2-Furin was assessed through a thermal shift assay, with increases in the temperature of a protein with a fluorescent dye along with it. As the protein denatures, the dye will bind to the amino acids and emit fluorescence, indicating when the protein unravels. A stable protein will have a defined peak in this range of temperatures to indicate its ideal state. If a peak is not defined, that could indicate an improperly folded protein. The Thermal Shift Assay of MMP-2-Native can be seen below in Figure 21.

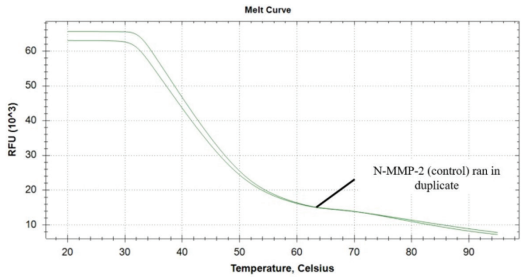

Figure 21: This figure is a graph of the Thermal Shift Assay of MMP-2-Native as described above. RFU stands for relative fluorescent units.

Since MMP-2-Native had no defined peak, the study determined that the protein could be unstable. This resulted in the study supplementing the protein with zinc and calcium ions since they were structural ions that were missing in the expression feeds, leading to unstable protein. The study predicted that the addition of these ions could induce spontaneous folding. The Thermal Shift Assay was run again with the MMP-2-Native and MMP-2-Furin, both before and after ion supplementation. This can be seen below in Figure 22.

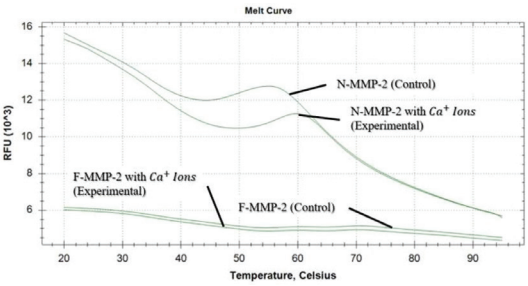

Figure 22: This figure is a graph of the Thermal Shift Assay of MMP-2-Native and MMP-2-Furin as described above. RFU stands for relative fluorescent units.

The supplementation of ions resulted in a more defined curve for MMP-2-Native, but MMP-2-Furin still seems unstable and denatured. Despite unideal conditions, the study moved forward with enzyme activity assays since any doubts on protein stability can be answered if the study could see whether the protein is enzymatically active.

The MMP-2 protein is a protease, meaning that its enzymatic activity involves cutting other proteins. This led the study to use a fluorogenic substrate identified in the methodology, which would typically be cleaved by MMP-2 and, in turn, release fluorescence. The MMP-2-Furin protein was activated with Furin. The MMP-2-Native protein is activated using Tween-20 (detergent) and a reducing agent (DTT) to reduce the thiol group between the propeptide and the native sequence. The enzyme activity assays for both MMP-2-Furin and MMP-2-Native can be seen, respectively, in Figure 23 and Figure 24 below.

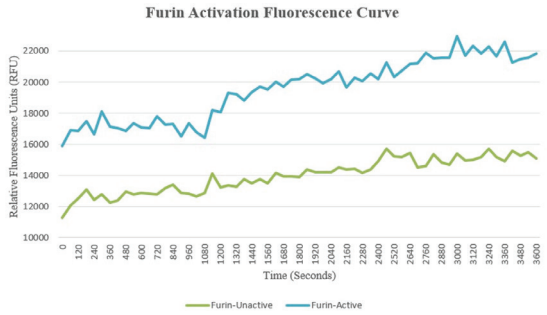

Figure 23: This figure is a graph of the enzyme activity assay of MMP-2-Furin as described above. RFU stands for relative fluorescent units.

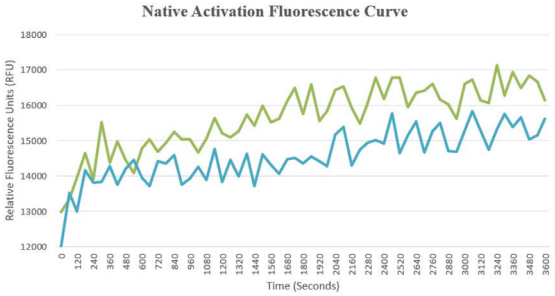

Figure 24: This figure is a graph of the enzyme activity assay of MMP-2-Native as described above. RFU stands for relative fluorescent units.

The increase in RFU may show that both MMP-2-Furin and MMP-2-Native, though to different degrees, were active and properly produced. This also validates that the novel activation mechanism that the study used with the MMP-2-Furin protein might be functional. The enzymatic kinetics of this activity assay need to be further validated with further in vitro testing in order to have sufficient evidence of activation.

Future Works:

In the future, the study plans on conducting the IC50 assay in combination with the active MMP-2 proteins and the fluorogenic substrate to measure the decrease in relative fluorescence emitted, as stated in the methodology. Crystallization of proteins will allow the study to analyze the structure of the protein and how it interacts with the inhibitory compound. This crystallization and x-ray diffraction will occur using known crystallization methods of the MMP-2 protein.[9] The study also plans to crystallize the inactive and active versions of

DOI: 10.36838/v8i3.76

MMP-2-Furin and MMP-2-Native. The crystallization will also be attempted with the MMP-2 active protein in complex with all tested inhibitors. This allows the study to find definitive answers on the effectiveness of various MMP-2 inhibitors in the context of hEDS disease. Further adaptations of this research would include *in vivo* effectiveness in mammalian cells to see if the MMP-2 inhibitors have the anticipated effect, which was hypothesized in the context of hEDS.

Conclusion

This study aimed to develop a therapeutic relief drug for hypermobile Ehlers-Danlos Syndrome (hEDS). Through literature review and research, it was revealed that the MTHFR gene mechanism mutation could be the leading cause of hEDS symptoms. This study chose to target a specifically overexpressed portion of this mechanism, which was the MMP-2 protein. The study analyzed various small-molecule inhibitors to help inhibit the activity of MMP-2 and regulate its function in hEDS patients to provide relief from hEDS symptoms. The study successfully identified 15 potential drug candidates or MMP-2 inhibitors computationally. The study also developed a novel activation mechanism for the MMP-2 protein using a Furin enzyme cleavage site for ease of use in *in vitro* settings. This successful identification of MMP-2 inhibitors and *in vitro* expression of the MMP-2 protein will allow future researchers to validate the study's results and potentially develop a drug utilizing the hypothesis developed in the study.

Acknowledgments

I would like to thank my adult sponsor, Mark Hayden, for allowing me to participate in the Central Bucks School District Biotechnology Partnership Program. I would like to thank my family and my sister for their help in encouraging me. I would also like to thank my mentors, Ryan Ford and Scott Willett, for being patient, guiding me, and educating me through this process.

References

1. The Ehlers-Danlos Society. hEDS Body System. The Ehlers-Danlos Society. https://www.ehlers-danlos.com/heds/.
2. Grahame, R. Joint Hypermobility and Genetic Collagen Disorders: Are They Related? *Arch. Dis. Child.* **1999**, *80* (2), 188–191. DOI: 10.1136/adc.80.2.188.
3. Mayo Clinic. Ehlers-Danlos Syndrome - Symptoms and Causes. Mayo Clinic. https://www.mayoclinic.org/diseases-conditions/ehlers-danlos-syndrome/symptoms-causes/syc-20362125.
4. Malfait, F.; Francomano, C.; Byers, P.; Belmont, J.; Berglund, B.; Black, J.; Bloom, L.; Bowen, J. M.; Brady, A. F.; Burrows, N. P.; et al. The 2017 International Classification of the Ehlers-Danlos Syndromes. *Am. J. Med. Genet. C Semin. Med. Genet.* **2017**, *175* (1), 8–26. DOI: 10.1002/ajmg.c.31552.
5. Demmler, J. C.; Atkinson, M. D.; Reinhold, E. J.; Choy, E.; Lyons, R. A.; Brophy, S. T. Diagnosed Prevalence of Ehlers-Danlos Syndrome and Hypermobility Spectrum Disorder in Wales, UK: A National Electronic Cohort Study and Case–Control Comparison. *BMJ Open* **2019**, *9* (11), e031365. DOI: 10.1136/bmjopen-2019-031365.
6. Courseault, J.; Kingry, C.; Morrison, V. E.; Edstrom, C.; Morrell, K.; Jaubert, L.; Elia, V.; Bix, G. J. Folate-Dependent Hypermobility Syndrome: A Proposed Mechanism and Diagnosis. *Heliyon* **2023**, *9* (4), e15387. DOI: 10.1016/j.heliyon.2023.e15387.
7. Ehlers-Danlos News. Mutations That Impair Folate Processing May Be Cause of Hypermobile EDS. https://ehlersdanlosnews.com/news/mutations-impair-folate-processing-cause-hypermobile-study/?cn-reloaded=1.
8. ThermoFisher. *ExpiCHOTM Expression System: User Guide*; 2018. https://assets.thermofisher.com/TFS-Assets/LSG/manuals/MAN0014337_expicho_expression_system_UG.pdf.
9. Morgunova, E. Structure of Human Pro-Matrix Metalloproteinase-2: Activation Mechanism Revealed. *Science* **1999**, *284* (5420), 1667–1670. DOI: 10.1126/science.284.5420.1667.
10. Zimmer, G.; Conzelmann, K.-K.; Herrler, G. Cleavage at the Furin Consensus Sequence RAR/KR(109) and Presence of the Intervening Peptide of the Respiratory Syncytial Virus Fusion Protein Are Dispensable for Virus Replication in Cell Culture. *J. Virol.* **2002**, *76* (18), 9218–9224. DOI: 10.1128/jvi.76.18.9218-9224.2002.
11. KTH Royal Institute of Technology. IMAC - Immobilized Metal-Affinity Chromatography. https://static.igem.org/mediawiki/2017/a/a6/Stockholm_IMAC.pdf.
12. Caers, J.; Van Der Juegt, B. Quantification of Proteins by UV-Vis Absorbance Using VICTOR Nivo with Microvolume Plates. https://resources.revvity.com/pdfs/app-quantification-of-proteins-by-uvvis-absorbance-using-victor-nivo.pdf (accessed 2025-06-20).
13. SDS-PAGE. Assay Protocol. http://www.assay-protocol.com/molecular-biology/electrophoresis/denaturing-page.html.
14. Schrödinger. Maestro. Life Science Content Library. https://www.schrodinger.com/life-science/resources/ (accessed 2025-06-20).
15. SwissADME. SwissADME. http://www.swissadme.ch/.
16. RCSB Protein Data Bank. Crystal Structure of Human MMP-2 Catalytic Domain in Complex with Inhibitor. *RCSB PDB* https://www.rcsb.org/structure/7XGJ (accessed 2025-06-20).
17. Coscueta, R.; Pintado, M. M. ACE-Inhibitory Activity Assay: IC50 V1. *protocols.io* **2022**. DOI: 10.17504/protocols.io.q26g74q5kgwz/v1.
18. Bio-Rad. Protein Thermal Shift. https://www.bio-rad.com/webroot/web/pdf/lsr/literature/Bulletin_7180.pdf.
19. Knight, C. G.; Willenbrock, F.; Murphy, G. A Novel Coumarin-Labelled Peptide for Sensitive Continuous Assays of the Matrix Metalloproteinases. *FEBS Lett.* **1992**, *296* (3), 263–266. DOI: 10.1016/0014-5793(92)80300-6.
20. Fields, G. B. Using Fluorogenic Peptide Substrates to Assay Matrix Metalloproteinases. *Methods Mol. Biol.* **2010**, 393–433. DOI: 10.1007/978-1-60327-299-5_24.
21. Sigma-Aldrich. Benzil. *Merck* **2025**, *1* (1).
22. Phizicky Lab. Measuring Nucleic Acid/Protein Concentration with NanoDrop 1000 V3.6 Spectrophotometer. https://www.urmc.rochester.edu/MediaLibraries/URMCMedia/labs/kielkopf-lab/documents/nanodrop2022update.pdf.
23. Binding Database. Type IV Collagenase 72kDa. https://www.bindingdb.org/rwd/jsp/dbsearch/PrimarySearch_ki.jsp?tag=pol&submit=Search&target=72%20kda%20type%20iv%20collagenase&polymerid=112,8378,10557,50001223.

Authors

Shreejith Krishnamoorthy is a passionate student at Central Bucks High School South. He is interested in the interdisciplinary field between biotechnology and business. He hopes to

be involved in biotech start-ups that can help patients with rare diseases, such as Ehlers-Danlos Syndrome, get the attention and research that they deserve.

DOI: 10.36838/v8i3.76